# Bandwidth Enhancement of Single-feed Circularly Polarized Antenna using Meta-surface

Nasimuddin, *Senior Member IEEE*, Zhi Ning Chen, *Fellow IEEE*, and Xianming Qing, *Member IEEE*

*Abstract* — **A single-feed circularly polarized (CP) rectangular slotted-patch antenna with meta-surface is proposed for bandwidth enhancement. The antenna consists of a rectangular slotted-patch radiator, a meta-surface with an array of rectangular-ring cells, and a coaxial feed. Utilization of the meta-surface achieves a wide CP bandwidth of seven times of the conventional antenna. The measured 3-dB axial ratio bandwidth of an antenna prototype printed onto a FR4 substrate is 28.3% (3.62 GHz–4.75 GHz) with 2:1-VSWR bandwidth of 36%. A 6.0-dBic boresight gain with variation of 1.5 dB is achieved across the frequency band of 3.35 GHz–4.75 GHz with the maximum gain of 7.4 dBic at 4.1 GHz.**

***Index Terms*** — Circularly polarized, low-profile, microstrip, meta-surface, rectangular patch, single-feed, slotted-patch antenna, wideband

## I. Introduction

A low-profile, wideband, CP antenna is desired for wireless systems. Generally, a single-feed CP microstrip antenna is with a simple configuration but suffers from a narrow axial ratio (AR) bandwidth. The bandwidth of a multiple-feed CP microstrip antenna can be enhanced while a complicated and larger feeding network is required. Many techniques have been employed to improve the AR bandwidth such as using dual-feed network based structures [1], stacked patches [2-3], array antennas with sequential feeding network [4], and multilayered structures [5]. However, these CP antennas are based on multi-radiating patches or complicated feeding structures.

Meta-surface is a two-dimensional structure and has been applied to design of the CP microstrip antennas (CPMAs) for miniaturization and performance enhancement [6-8]. In [6], reactive impedance surface (RIS) and mushroom-shaped structure have been used to miniaturize the CPMA. The antenna is designed on a thick dielectric substrate with low gain of 2.98 dBic and narrow 3-dB AR bandwidth of 1.46%. In [7], the miniaturization of the CPMA is achieved using RIS with complementary split-ring resonators. The antenna gain is 3.7 dBic with a narrow 3-dB AR bandwidth of 1.1%. A single-feed meta-surface based CPMA with compact size was proposed in [8] with a 3-dB AR bandwidth of 2.33%. A number of RIS-based microstrip antennas have been proposed and studied in [9], wherein, the CPMAs are with the largest 3-dB AR bandwidth of 2.4%.

On the other hand, a single dipole antenna over an artificial ground plane based on the polarization dependent electromagnetic band gap (EBG) surface was studied and a 3-dB AR bandwidth of 5.6% is achieved [10]. In [11], the RIS structures have been investigated for CPMA design and a 3-dB AR bandwidth of 10.6% is demonstrated. Recently, an artificial magnetic conductor (AMC) surface has been used as the reflector of a CP slot antenna to generate a wideband unidirectional CP radiation [12]. The polarization dependent EBG surface has been detailed studied in [13] for microstrip antenna design applications.

In this paper, a meta-surface based single-feed CP rectangular slotted-patch antenna is investigated for bandwidth enhancement. A 7x7 rectangular-ring unit cells based meta-surface is used to enhance the bandwidth. The antenna prototype is measured and compared with simulation using the CST Microwave Studio [14]. Parametric studies are carried out to understand of the operation mechanism of the proposed antenna.

## II. Antenna Geometry and Design

Fig. 1 shows the configuration of the proposed wideband CPMA. The antenna is oriented such that the center of the rectangular patch is at the origin of the coordinate. It consists of a rectangular patch with a circular-ring-slot along the $x$-axis, a meta-surface, and a coaxial feed. As shown in Fig. 1(c), the meta-surface consists of an array of 7×7 rectangular-ring unit cells.

The meta-surface is positioned at a height of $h_1$ = 3.2 mm on a FR4 substrate (dielectric constant, $\varepsilon_r$ = 4.3 and loss tangent of 0.02). The rectangular slotted-patch radiator is placed on the top layer of the FR4 substrate and above the meta-surface with the thickness of $h_2$ = 1.6 mm. The antenna is designed to achieve a wideband CP radiation across an operating frequency band of 3.6 GHz–4.8 GHz. The dimensions of the optimized antenna are: ground plane length/width: 88 mm/60 mm, radiating patch: $L_p$ = 15.12 mm, $W_p$ = 11.5 mm (aspect ratio, $Ar_p$ = 1.315), embedded ring-slot in the rectangular radiating patch: $r_1$ = 2.6 mm, $r_2$ = 1.9 mm, embedded ring-slot location in rectangular patch = $L_p/4$, 0, meta-surface with 7×7 rectangular-ring unit cells: length, $L_u$ = 8.96 mm, width, $W_u$ = 5.6 mm, $S_l$ = 7.46 mm, and $S_w$ = 0.85 mm (unit cell size: 0.075 $\lambda_o$×0.119 $\lambda_o$, where $\lambda_o$ is the free space wavelength at 4 GHz), distance between the unit cells in $x$-direction, $d_x$ = 1.52 mm, distance between the unit cells in $y$-direction: $d_y$ = 1.26 mm, the coaxial feed location: $x_p$ = 6.2

The work was supported by Economic Development Board (EDB), Singapore, under the office for space technology and industry (OSTIn) Space Industry Alignment Grant ("SIAG") S14-1139-IAF OSTIn-SIAG.

Authors are with the Institute for Infocomm Research, A*STAR, 1 Fusionopolis Way, #21-01 Connexis (South Tower), Singapore 138632. (e-mail: nasimuddin@i2r.a-star.edu.sg, chenzn@i2r.a-star.edu.sg, qingxm@i2r.a-star.edu.sg).

Zhi Ning Chen is also with Department of Electrical and Computer Engineering, National University of Singapore (eleczn@nus.edu.sg).

mm, $y_p$ = 4.0 mm ($\theta$ = 33°), and overall antenna size: 60.0 mm × 88.0 mm × 4.8 mm.

A ring-slot in the rectangular patch radiator is able to shift down the lower edge of the 3-dB AR frequency range. To avoid possible contact between the coaxial feed and the unit cells of the meta-surface, a circular area with a radius of 1.85 mm is cut onto the meta-surface. The proposed rectangular slotted-patch antenna is left-hand CP when its feeding point is positioned close to the diagonal line with the coordinate of ($-x_p$, $-y_p$) or ($x_p$, $y_p$). A right-hand CP will be generated when the feeding point is positioned close to the other diagonal line with the coordinate of ($-x_p$, $y_p$) or ($x_p$, $-y_p$).

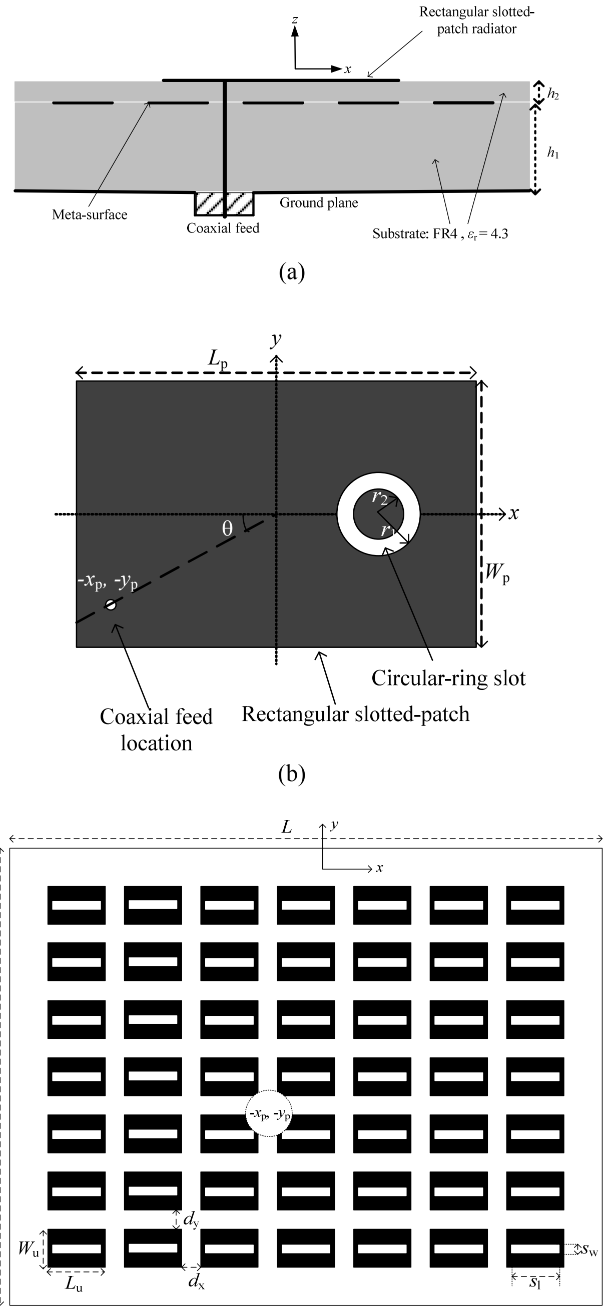


Fig. 1. Proposed meta-surface based wideband CP rectangular patch antenna: (a) cross-sectional view, (b), rectangular slotted-patch radiator, and (c) meta-surface with a 7x7 rectangular-ring unit cells.

*A. Operating Mechanism*

The operating principle of the proposed CPMA is studied as follows. Generally, the square slotted/slit/truncated-patch and nearly-square patch antennas have been used to generate the narrow band CP radiation. In proposed antenna design, the rectangular slotted-patch antenna over meta-surface is used to generate the wideband CP radiation. The field distributions on the rectangular slotted-patch antenna are shown in Figs. 2(a)-2(e), respectively, at $\omega t$ = 0°, 45°, 90°, and 135°. A time dependent circularly rotated field distribution is observed, which suggests that the proposed antenna is able to generate a CP radiation.

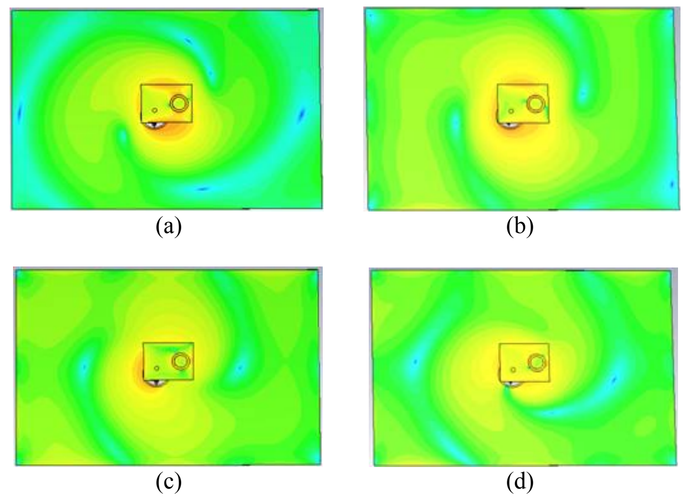


Fig. 2. Field distributions of the proposed rectangular slotted-patch antenna: (a) $\omega t$ = 0°, (b) $\omega t$ = 45°, (c) $\omega t$ = 90°, and (d) $\omega t$ = 135°.

*B. Unit Cell of Metamaterial-surface*

The reflection phase response of the unit cell is studied as shown in Fig. 3. The phase crosses through the range of +90° and −90° across a wide frequency range. This provides a useful reference to determine the operating frequency band of the meta-surface for wideband antenna design [15]. The frequency range of the proposed rectangular-ring unit cell within ±90° reflection phase variation is from 1.8 GHz to 4.8 GHz, which suggests the meta-surface using the proposed unit cell is desirable for wideband antenna design.

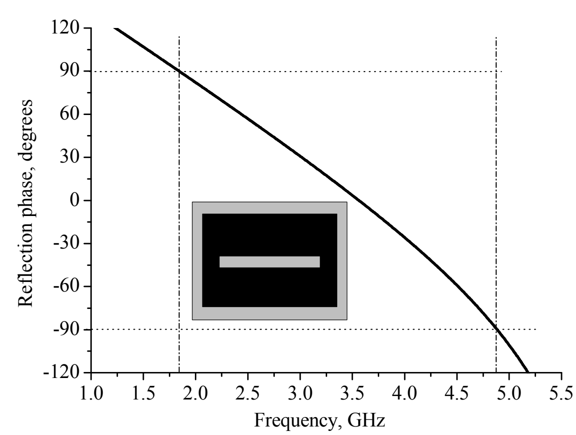


Fig. 3. Reflection phase diagram of the meta-surface unit cell.

### C. *Antenna with and without meta-surface*

Utilization of the meta-surface widens operating bandwidth and enhances the gain of the proposed antenna. The reason can be attributed two factors. One is that positioning the meta-surface underneath the patch radiator results in additional electromagnetic coupling between the patch and the meta-surface so that the operating bandwidth is enhanced. The other one is that the meta-surface improves the field distribution of the antenna so that the effective aperture of the antenna is enlarged.

Fig. 4 compares the performance of the antennas in terms of impedance, axial ratio, and gain, where the reference antenna without the meta-surface is with the same configuration and dimensions as the proposed antenna. It is seen clearly that the meta-surface improves the VSWR<2:1, 3-dB AR bandwidths, and gain. The VSWR<2:1 bandwidth of the antenna with the meta-surface reaches 35.6% (3.22 GHz–4.63 GHz) while the reference antenna realizes 20.8% (4.11 GHz–5.05 GHz) only. Also, the meta-surface improves the 3-dB AR bandwidth around seven times when compared with the reference antenna. The 3-dB AR bandwidth of the antenna with and without meta-surface is 28.6% (3.58 GHz–4.72 GHz) and 4.25% (4.17 GHz–4.35 GHz), respectively. The gain is enhanced about 3-dB by the meta-surface. Fig. 5 shows that the proposed antenna realizes the uniform field distributions when compared with the reference antenna (Fig. 2) which helps to enlarge the effective aperture of the proposed antenna.

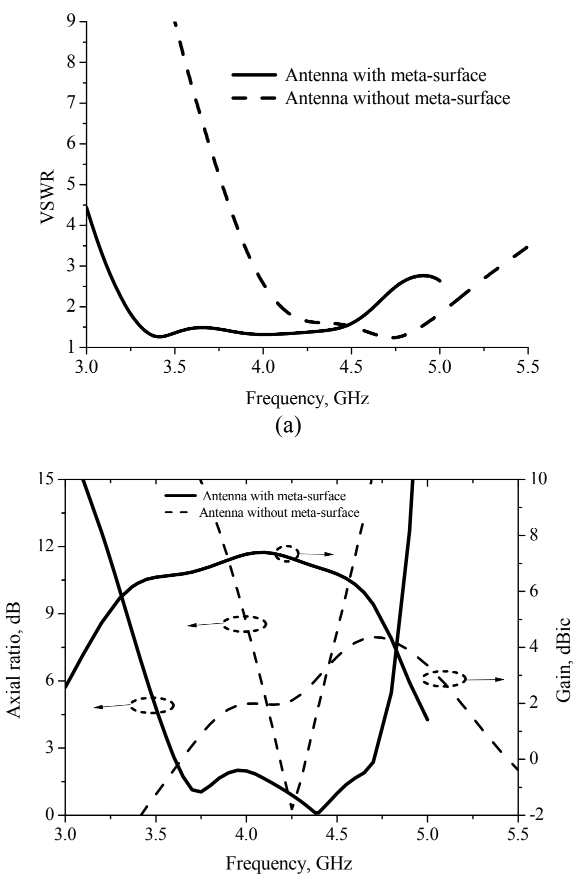

(a)

(b)

Fig. 4. Performance comparison of the antenna with and without meta-surface: (a) VSWR and (b) AR and gain at the boresight.

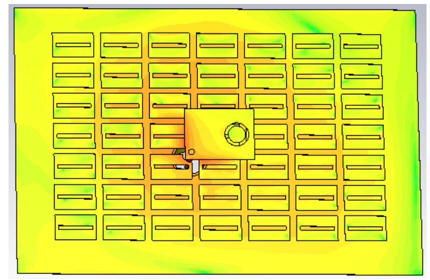

Fig. 5. Field distributions on antenna with meta-surface.

## III. Parametric Study

The parametric studies are carried out by simulation wherein only one parameter is changed each time while the others are kept unchanged. The antenna design dimensions shown in Section II are used as the reference.

### A. *Number of unit cells for meta-surface*

Fig. 6 shows the 3-dB AR bandwidth and 1-dB gain variation bandwidth with varying number of the unit cell of the meta-surface. It is observed that the 3-dB AR bandwidth is sensitive to the number of unit cells and reaches the maximum of 28% when the meta-surface is with unit cell array of 7×7. When the number of the unit cell is zero, namely, the antenna is without meta-surface; the 3-dB AR bandwidth is only around 4.3%. However, besides the meta-surface with unit cell arrays of 6×6 or 7×7, the proposed antenna shows almost the same 3-dB AR bandwidth of the antenna without meta-surface. The 1-dB gain bandwidth shows a similar trend with less variation. The following parametric studies will be carried out based on the meta-surface of 7×7 unit cell array.

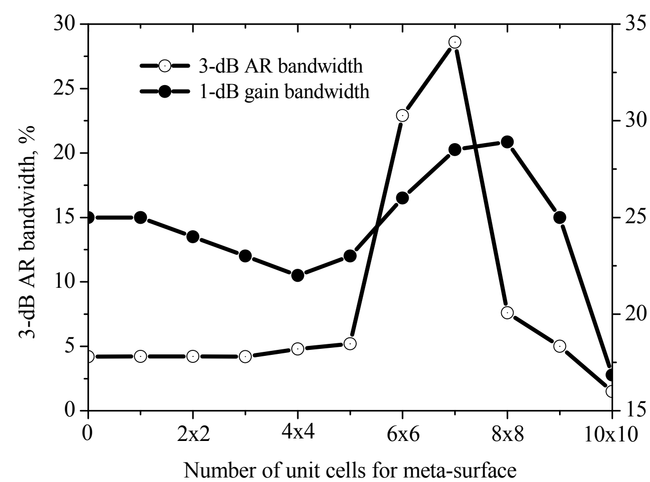


Fig. 6. 3-dB AR bandwidth and 1-dB gain bandwidth with variation of number of the unit cells for the meta-surface.

### B. *Aspect-ratio of rectangular-ring unit cell, $Ar_u$*

The variation of the AR at the boresight with varying aspect-ratio of the unit cell is shown in Fig. 7. It is found that the $Ar_u$ shows significant effect on the 3-dB AR bandwidth. When $Ar_u$ = 1.6, the largest 3-dB AR bandwidth is achieved. When $Ar_u$ = 1 (square-ring unit cell for meta-surface), the AR becomes poor and the bandwidth reduce dramatically.

*C. Spacing between rectangular-ring unit cell, $d_x$ and $d_y$*

The spacing between the unit cells of the meta-surface in *x*- and *y*-axes also affects the performance of the antenna. The AR variation across a frequency band with different spacing between unit cells in *x*- and *y*-direction, $d_x$ and $d_y$, are illustrated in Figs. 8 and 9 respectively. The $d_x$ affects the 3-dB AR bandwidth of the proposed antenna more than the $d_y$. The widest 3-dB AR bandwidth is achieved as $d_x$ = 1.52 mm and $d_y$ = 1.26 mm.

*D. Aspect-ratio of patch radiator, $Ar_p$*

The AR at the boresight with varying aspect ratio of the patch radiator, $Ar_p$, is plotted in Fig. 10. The widest 3-dB AR bandwidth is achieved with $Ar_p$ = 1.32. The AR is degraded and 3-dB AR bandwidth is narrowed when $Ar_p$ diverges from 1.32. When $Ar_p$ = 1, the AR is more than 6 dB across the desired bandwidth, It indicates that the single-feed slotted square patch over the proposed meta-surface is unable to generate the two orthogonal modes with an equal magnitude for CP radiation.

*E. Coaxial Feed Location*

The location of the feeding point is with the coordinate of ($-x_o\times\cos(\theta)$, $-x_o\times\sin(\theta)$), where $x_o$ = 7.35 mm. As shown in Fig. 11, the location of the feeding point exhibits significant effect on the AR of the antenna. When the feeding point is close to the diagonal line of the patch ($\theta$ = 33°), the wideband CP radiation (3-dB AR bandwidth) can be achieved. If the feeding point is positioned apart from the diagonal line, the orthogonal modes with an equal magnitude and a 90° phase shift are unable to be maintained so that the CP radiation cannot be generated.

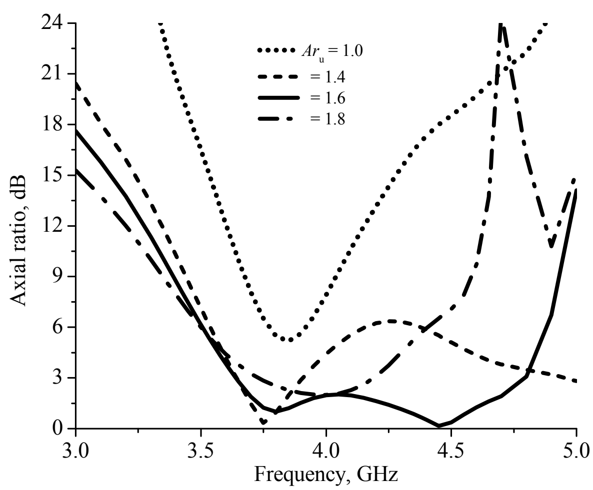


Fig. 7. Axial ratio at the boresight with variation of unit cell aspect-ratio.

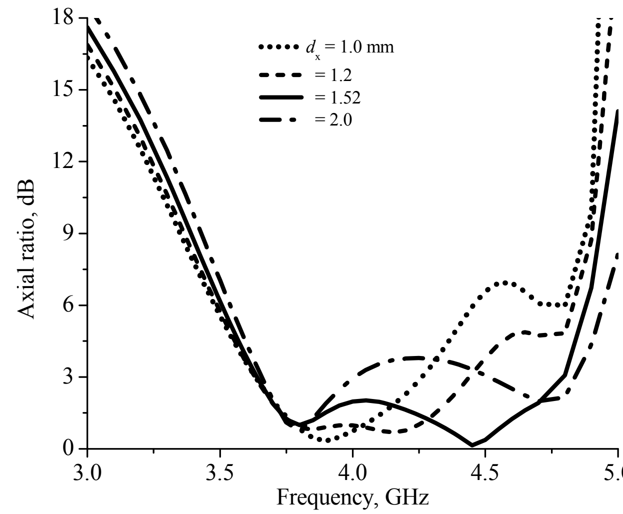


Fig. 8. Axial ratio at the boresight with variation of distance between unit cells in *x*-axis direction ($d_x$).

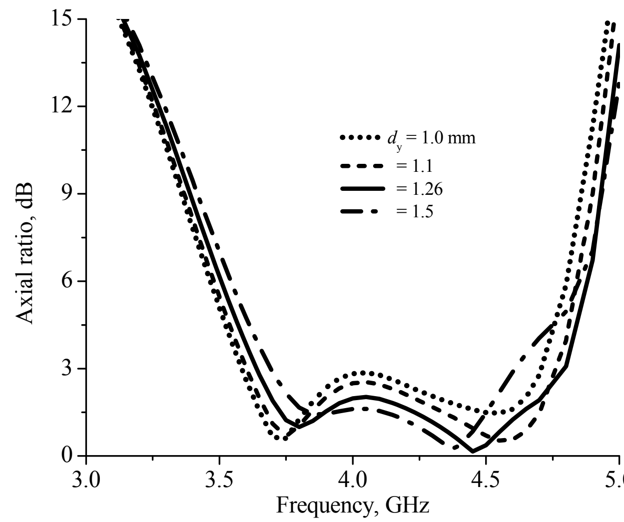


Fig. 9. Axial ratio at the boresight with variation of distance between unit cells in *y*-axis direction ($d_y$).

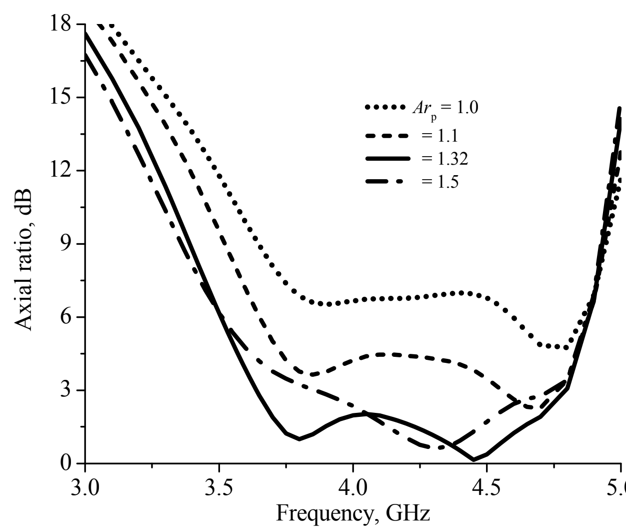


Fig. 10. Axial ratio at the boresight with variation of patch radiator aspect-ratio.

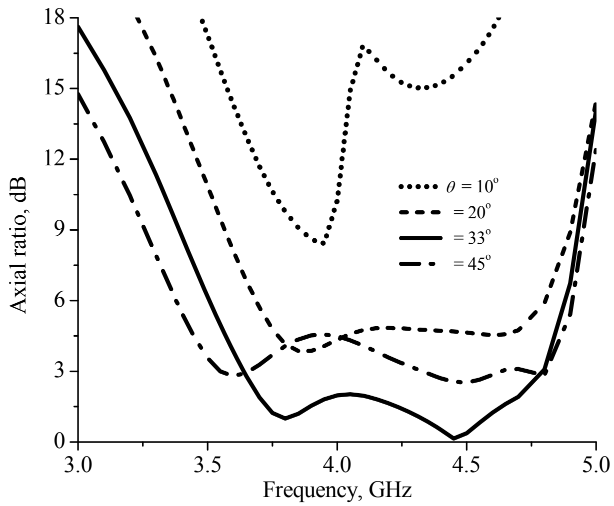


Fig. 11. Axial-ratio at the boresight with variation of coaxial feed location angle ($\theta$).

The design guideline of the proposed antenna is summarized as follows,

a) Determine the initial dimensions of the rectangular patch radiator according to the operating frequency, dielectric material, and antenna size constraint;

b) Design unit cell for the meta-surface. The dimensions of the rectangular-ring unit cell should be $\leq \lambda_o/10$. A unit cell should be with a reflection phase response of $\pm 90^\circ$ exceeding the required operating frequency band;

c) Select the number of unit cells for meta-surface based on the requirements of gain and bandwidth;

d) Determine the position of the feeding point according to the requirement of the CP radiation; and

e) Optimize the antenna to achieve desired specifications.

## IV. Experimental Results and Discussions

The proposed antenna design was prototyped and measured in a full anechoic chamber using Midas 5.0 antenna measurement system. The photo of the prototype antenna is illustrated in Fig. 12. The simulated and measured 2:1-VSWR bandwidths are, respectively, 35.6% (3.22 GHz–4.63 GHz) and 36.0% (3.32 GHz–4.76 GHz) as shown in Fig. 13.

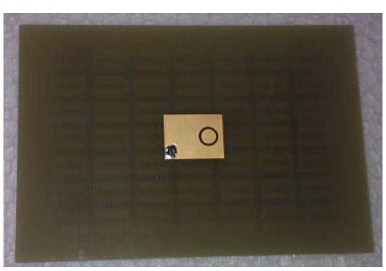

Fig. 12. Photo of prototype antenna.

The measured 3-dB AR bandwidth is 28.3% (3.62 GHz–4.75 GHz); a good agreement is achieved with the simulation as shown in Fig. 14. Fig. 15 compares the simulated and measured gain at the boresight. The measured 3-dB gain bandwidth is 40% (3.2 GHz–4.8 GHz) with maximum gain of 7.4 dBic at 4.1 GHz. The efficiency of the proposed antenna is also exhibited in Fig. 15 and it is greater than 70% across the 3-dB AR bandwidth. The measured and simulated normalized radiation patterns at 3.75 GHz and 4.25 GHz are plotted in Fig. 16 in both *xz*- and *yz*-planes, respectively. The simulated radiation pattern curves are in good agreement with the measured radiation patterns in both planes. The radiation patterns have been measured using a rotating linearly polarized horn antenna system [16]. The ripples in the patterns indicate the AR performance against the angle; the larger the ripple, the worse the AR.

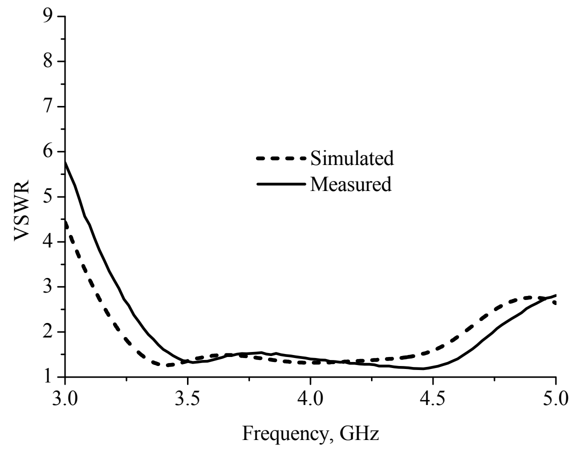


Fig. 13. Measured and simulated VSWR.

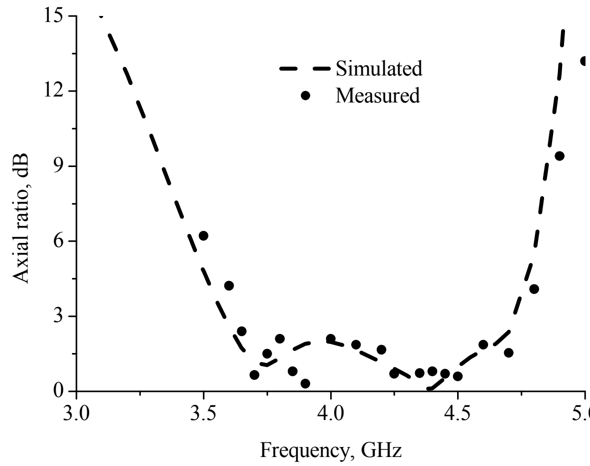


Fig. 14. Measured and simulated axial ratio at the boresight.

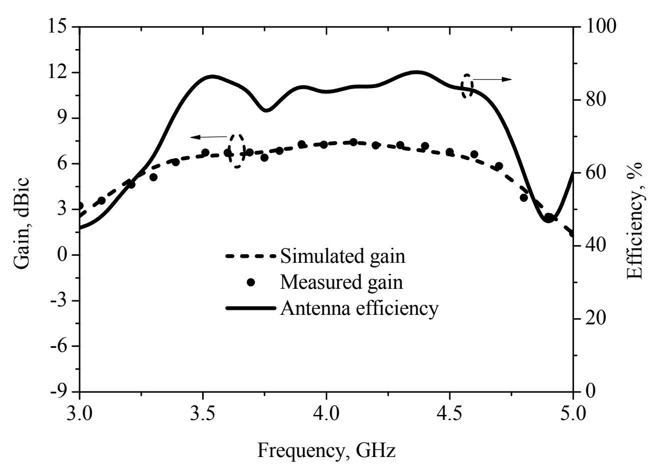


Fig. 15. Measured and simulated gain at the boresight with antenna efficiency.

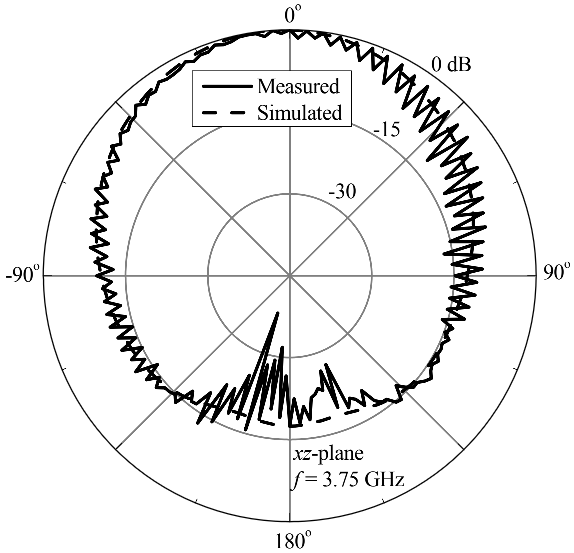


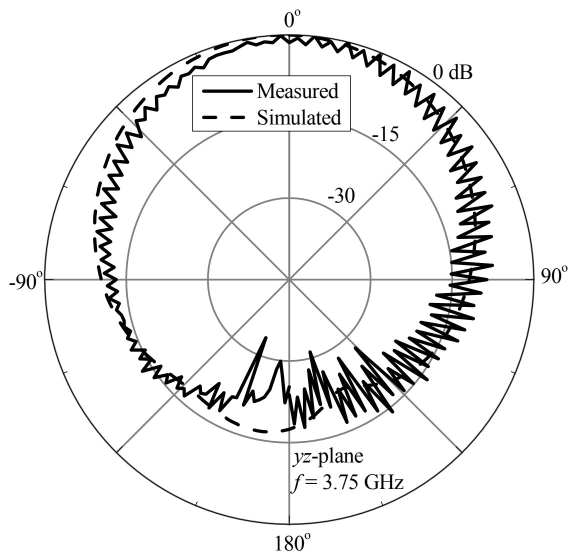


(a)

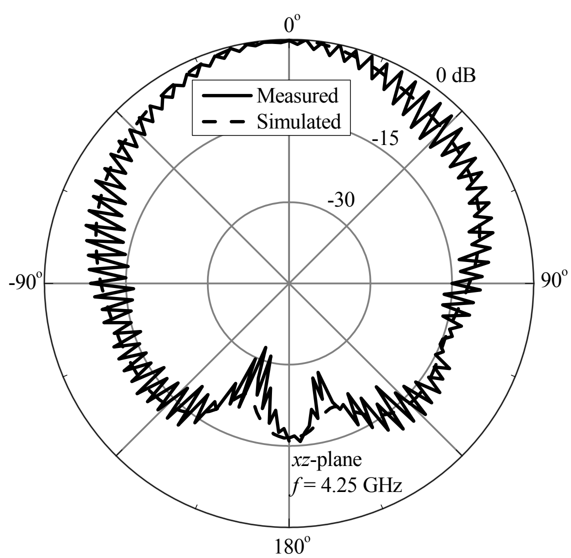


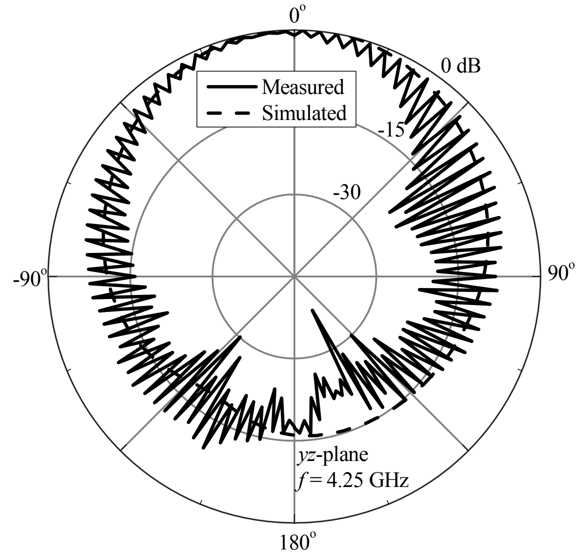


(b)

Fig. 16. Measured and simulated normalized radiation patterns in *xz*- and *yz*-plane: (a) 3.75 GHz and (b) 4.25 GHz.

The measured performances of the proposed antenna are tabulated in Table I and compared with related published designs using meta-surfaces in the literature [6-12]. It can be seen that the proposed antenna is able to generate CP radiation across a wider bandwidth with a lower profile configuration. The square patch antennas with composite right/left-handed (CRLH) mushroom/RIS/meta-surface published in Refs. [6-9] have compact antenna configurations but narrower 3-dB AR bandwidth. The dipole antenna over a meta-surface [10] can achieve the 3-dB AR bandwidth of 5.6% with the larger overall antenna volume. In Ref. [11], the patch antenna above a meta-surface was proposed with 3-dB AR bandwidth of 10.6%, which is narrower than that of the proposed antenna in this work.

TABLE II. COMPARISON OF MEASURED PERFORMANCES OF THE CPMAS OVER META-SURFACE

| Antenna configuration | 10-dB Return loss BW (%) | 3-dB AR BW (%) | Gain (dBic) | Overall Antenna volume |
|---|---|---|---|---|
| Antenna with CRLH mushroom structure & RIS [6] | 4.60 | 1.46 | 2.98 | $0.293\lambda_0 \times 0.293\lambda_0 \times 0.026\lambda_0$ at 2.58 GHz |
| Antenna with complementary split-ring resonators and RIS [7] | 4.90 | 1.68 | 3.7 | $0.327\lambda_0 \times 0.327\lambda_0 \times 0.028\lambda_0$ at 2.8 GHz |
| Antenna with meta-surface [8] | 2.33 | 2.33 | 5.1 | $0.435\lambda_o \times 0.435\lambda_o \times 0.019\lambda_o$ at 3.0 GHz |
| Truncated corners square patch over RIS [9] | 7.49 | 2.55 | 5.54 | $0.315\lambda_o \times 0.315\lambda_o \times 0.0333\lambda_o$ at 2.7 GHz |
| Dipole with meta-surface [10] | 24.0 | 5.6 | - | $1.163\lambda_o \times 1.163\lambda_o \times 0.106\lambda_o$ at 3.5 GHz |
| Square patch with meta-surface[11] | 14.0 | 10.6 | 2.5-5.7 | $0.77\lambda_o \times 0.77\lambda_o \times 0.06\lambda_o$ at 2.3 GHz |

| | | | | |
|---|---|---|---|---|
| Proposed antenna | 36.0 | 28.3 | 7.0-7.5 | $0.822\lambda_o \times 1.18\lambda_o \times 0.06\lambda_o$ at 4.0 GHz |

## V. Conclusion

A meta-surface based single-feed rectangular slotted-patch antenna has been demonstrated to achieve the wideband CP radiation. The parametric studies have shown that the 3-dB AR bandwidth is much dependent on the configuration of the meta-surface, the size of the patch radiator, and the location of the feeding point. Necessary design guideline has been also suggested for engineers. The proposed single-feed CP antenna is low-profile with wideband characteristics and desired for wideband wireless systems.

## References


[1] S. D. Targonski and D. M. Pozar, "Design of wideband circularly polarized aperture coupled microstrip antennas," *IEEE Trans. Antennas and Propagation*, vol. 41, no. 2, pp. 214–220, Feb. 1993.

[2] N. Herscovici, Z. Sipus, and D. Bonefacic, "Circularly polarized single-fed wide-band microstrip patch," *IEEE Trans. Antennas and Propagation*, vol. 51, no. 6, pp. 1277–1280, June 2003.

[3] Nasimuddin, K. P. Esselle, and A. K. Verma, "Wideband circularly polarized stacked microstrip antennas," *IEEE Antennas and Wireless Propagation Letters*, vol. 6, pp. 21–24, 2007.

[4] H. Oraizi and R. Pazoki, "Wideband circularly polarized aperture-fed rotated stacked patch antenna," *IEEE Trans. Antennas and Propagation*, vol. 61, no. 3, pp. 1048–1054, March 2013.

[5] S. Raut and A. Petosa, "GPS wideband circularly polarized microstrip antenna array," 3rd *European Conference on Antennas and Propagation*, pp. 2990–2993, March 2009.

[6] Y. Dong, H. Toyao, and T. Itoh, "Compact circularly polarized patch antenna loaded with metamaterial structures," *IEEE Trans. Antennas and Propagation*, vol. 59, no. 11, pp. 4329–4332, Nov. 2011.

[7] Y. Dong, H. Toyao, and T. Itoh, "Design and characterization of miniaturized patch antennas loaded with complementary split-ring resonators," *IEEE Trans. Antennas and Propagation*, vol. 60, no. 2, pp. 772−785, Feb. 2012.

[8] H. X. Xu, G. M. Wang, J. G. Liang, M. Q. Qi, and X. Gao, "Compact circularly polarized antennas combining meta-surfaces and strong space-filling meta-resonators," *IEEE Trans. Antennas and Propagation*, vol. 61, no. 7, pp. 3442−3450, July 2013.

[9] K. Agarwal, Nasimuddin, and A. Alphones, "RIS based compact circularly polarized microstrip antennas," *IEEE Trans. Antennas and Propagation*, vol. 61, no. 2, pp. 547–554, Feb. 2013.

[10] F. Yang and Y. Rahmat-Samii, "A low profile single dipole antenna radiating circularly polarized waves," *IEEE Trans. Antennas and Propagation*, vol. 50, no. 9, pp. 3083–3086, Sept. 2005.

[11] L. Bernard, G. Chertier, and R. Sauleau, "Wideband circularly polarized patch antennas on reactive impedance substrates," *IEEE Antennas and Wireless Propagation Letters*, vol. 10, pp. 1015−1018, 2011.

[12] K. Agarwal, Nasimuddin, and A. Alphones, "Wideband circularly polarized AMC reflector backed aperture antenna," *IEEE Trans. on Antennas and Propagation*, vol. 61, no. 3, pp. 1456–1461, March 2013.

[13] F. Yang and Y. Rehmat-Samii, "Polarization-dependent electromagnetic band gap (PDEBG) structures: designs and applications," *Microwave and Optical Technology Letters*, vol. 41, no. 6, pp. 439–444, June 2004

[14] CST Microwave Studio 2014.

[15] D. Sievenpiper, L. Zhang, R. F. J. Broas, N. G. Alexopolous, and E. Yablonovitch, "High impedance electromagnetic surfaces with a forbidden frequency band," *IEEE Trans. Microw. Theory Tech*., vol. 47, no. 11, pp. 2059–2074, Nov. 1999.

[16] B. Y. Toh, R. Cahill, and V. F. Fusco, "Understanding and measuring circular polarization," *IEEE Transactions on Education*, vol. 46, no. 3, pp. 313−318, Aug. 2003.